

Supporting Information for: Direct vs Delayed Triplet Energy Transfer from Organic Semiconductors to Quantum Dots and Implications for Luminescent Harvesting of Triplet Excitons

Victor Gray^{†,‡}, Jesse R. Allardice[†], Zhilong Zhang[†], Simon Dowland[†], James Xiao[†], Anthony Petty, II,[†] John E. Anthony,[†] Neil C. Greenham[†], Akshay Rao^{†*}

[†]Cavendish Laboratory, University of Cambridge, J. J. Thomson Avenue, Cambridge CB3 0HE, U.K.

[‡]Department of Chemistry - Ångström Laboratory, Uppsala University, Box 523, 751 20, Uppsala, Sweden

[†]Department of Chemistry, University of Kentucky, 161 Jacobs Science Building, Lexington Kentucky 40506-0174, United States

Table of Contents

Experimental methods	2
Chemicals.....	2
Quenching of ligand exchanged QDs	2
Ligand Coverage	2
Transient absorption of ligand exchanged QDs.....	3
Derivation of PLQE equation	5
Transient absorption of PM samples	5
Decomposition of Triplet and QD features.....	6
TA of 1.18 eV 1.30 eV QD/TET-CA and triplet formation.....	7
Kinetic modelling	8
Rate equations governing PM	8
Fitting procedure	9
Fitting results and error estimate	10
References.....	10

Experimental methods

Chemicals

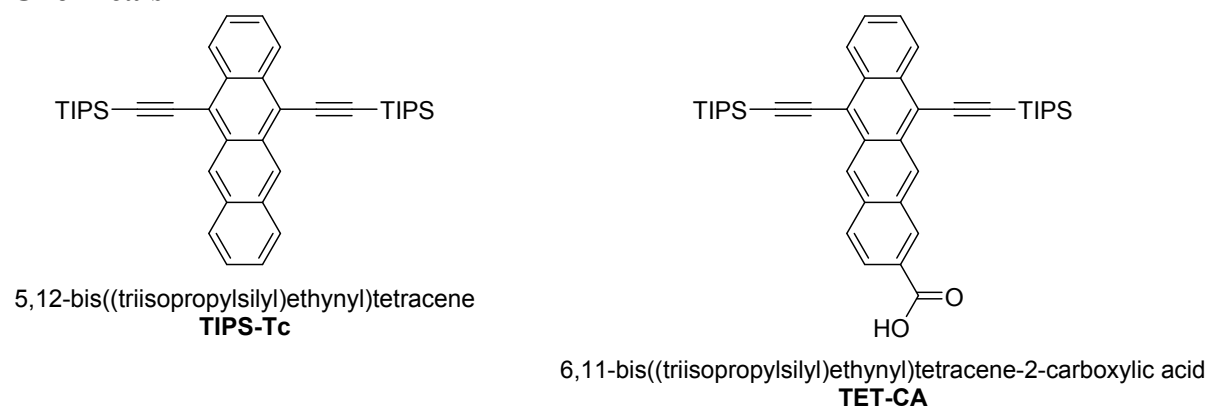


Figure S1. Molecular structures of the singlet-fission material **TIPS-Tc** (left) and the triplet transfer ligand **TET-CA** (right).

Quenching of ligand exchanged QDs

Ligand Coverage

Table 1. Properties of the synthesized PbS QDs.

Exciton Bandgap (eV)	Diameter (nm)	Size Distribution (%)	Ligand/QD	Ligand/nm ²
0.90	4.9	5.3	121.4	1.64
1.00	4.3	8.0	113.6	1.92
1.08	4.0	6.3	78.0	1.63
1.18	3.5	8.2	72.4	1.88
1.30	3.1	4.9	52.7	1.75

The ligand coverage was determined from UV-Vis absorption. The concentration of the PbS QD was estimated using the empirical formula for the molar absorptivity by Moreels *et al.*¹ The molar absorption coefficient of the ligand was determined to 25500 M⁻¹cm⁻¹ at the peak absorption in toluene.

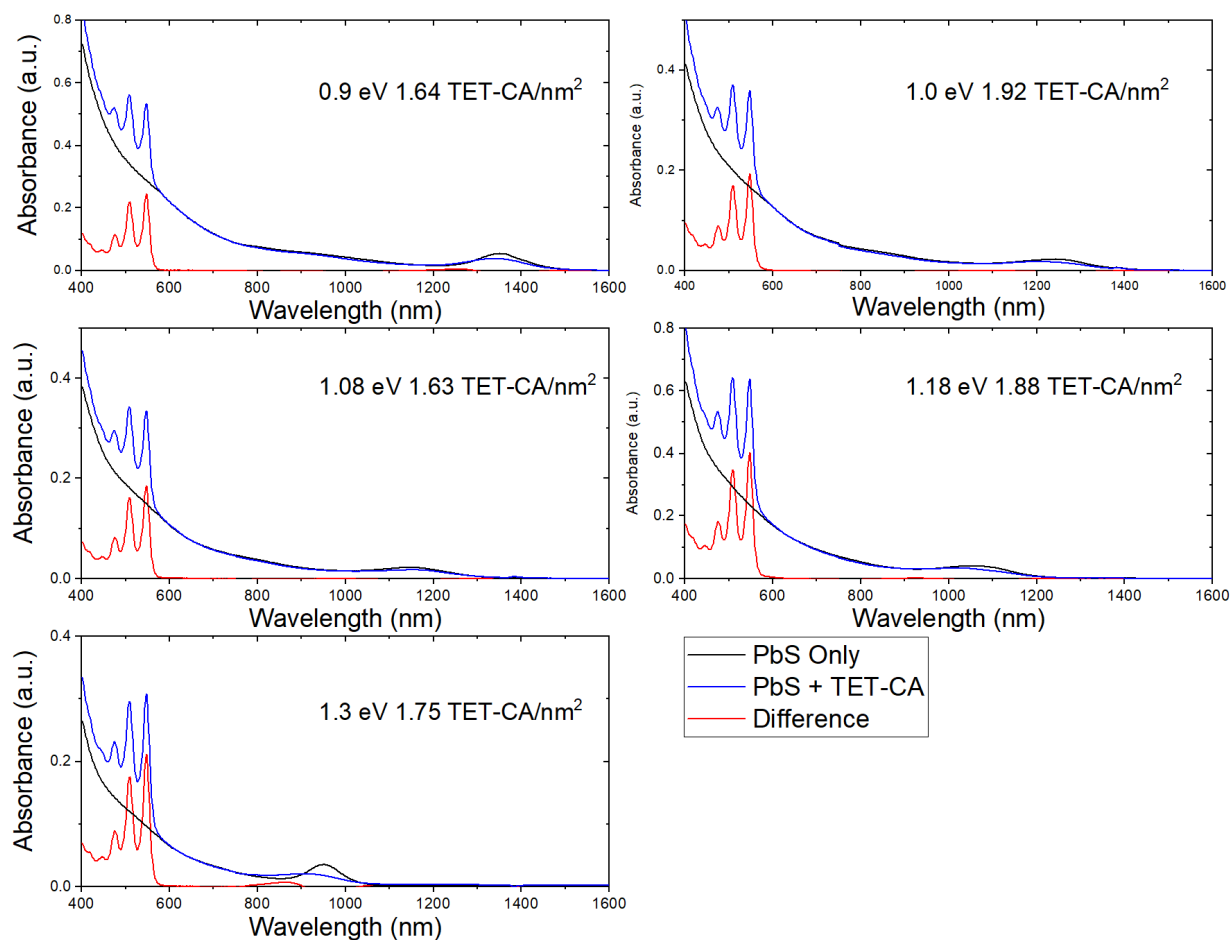


Figure S2. Absorption spectra of PbS QDs and PbS-QDs with TET-CA ligand in toluene, used to determine the ligand coverage.

Transient absorption of ligand exchanged QDs

Figure S3 shows the ps-resolved transient absorption kinetics of the PbS QDs. Before ligand exchange, the OA covered PbS QDs show no decay over the first 2 ns. After ligand exchange, a significant quenching occurs within a few 100 ps. To extract the fast component a biexponential fit was employed with a fixed second decay time of 1 μ s, except for the 1.3 eV QD where both decay constants were fitted.

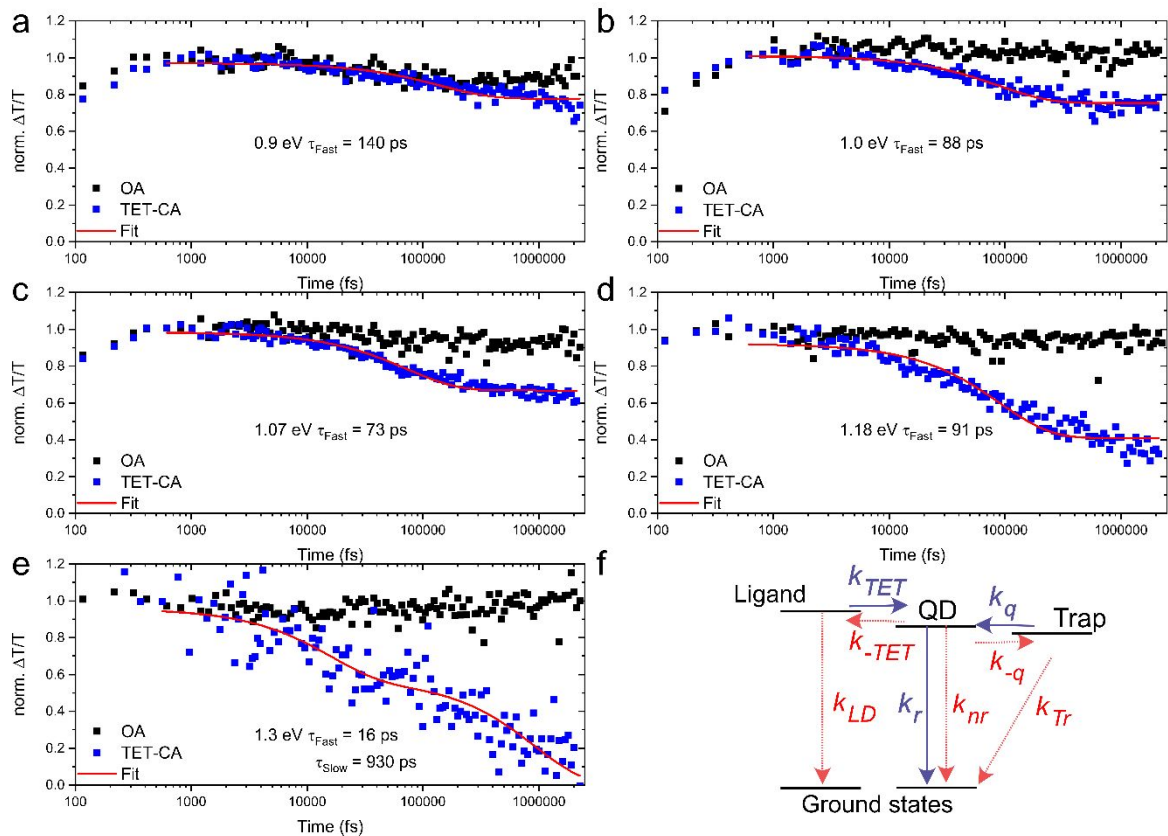


Figure S3. ps-Transient absorption kinetics of the PbS/OA and PbS/TET-CA QDs. Excitation wavelength was 658 nm with 5 nJ/pulses.

Figure S4 shows the kinetic traces in the nanosecond-microsecond time range, extracted from ns-TA measurements of OA ligated PbS QDs and TET-CA covered dots. The bimolecular lifetime of the 1.18 eV QD/TET-CA sample supports and equilibrium between ligand triplet and QD excited states, suggesting a close to isoenergetic energy alignment.

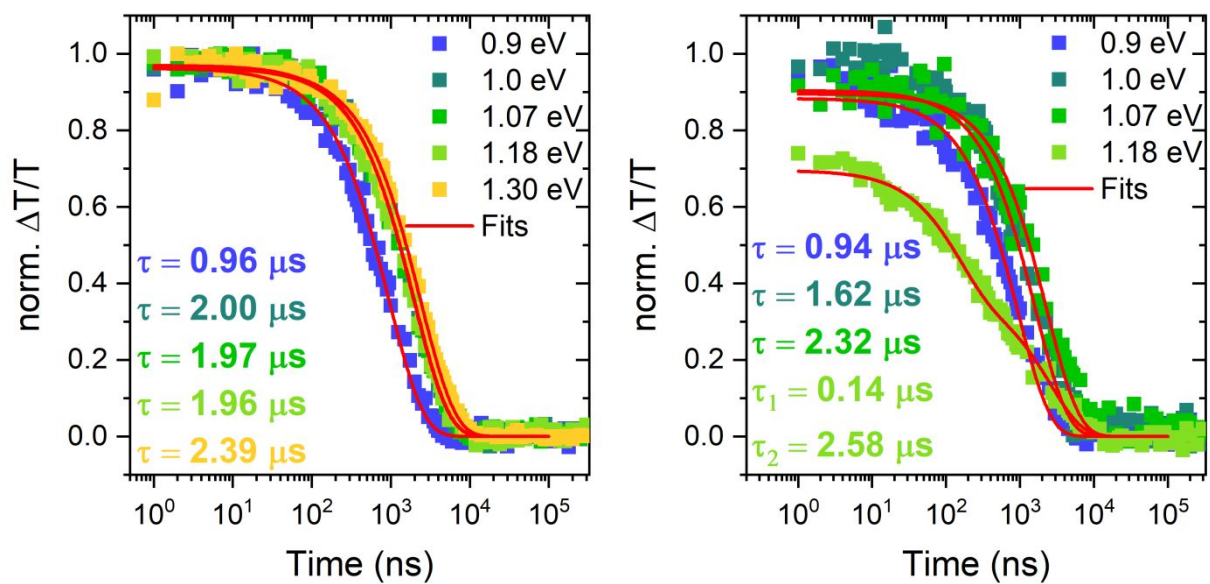


Figure S4. ns-Transient absorption kinetics of PbS/OA (left) and PbS/TET-CA QDs (right). Excitation at 550 nm with 45 nJ/pulses.

Derivation of PLQE equation

In Figure S4f a three state model where a QD exciton can decay intrinsically (k_{QD}) or by transfer to a trap state (Tr) or to a ligand state (L) with rates k_q and k_{TET} , respectively, is depicted. The QD can also be repopulated by the trap and ligand states with rates k_{-q} and k_{TET} , respectively. Such a three state model can be described by the following three rate equations:

$$\frac{d[QD]}{dt} = G - k_q[QD] + k_{-q}[Tr] - k_{-TET}[QD] + k_{TET}[L] - k_{QD}[QD] \quad (S1)$$

$$\frac{d[L]}{dt} = k_{-TET}[Q] - k_{TET}[L] - k_{LD}[L] \quad (S2)$$

$$\frac{d[Tr]}{dt} = k_q[QD] - k_{-q}[Tr] - k_{Tr}[Tr] \quad (S3)$$

Where G is the generation rate for exciting the QD to the excited state. The intrinsic QD decay, k_{QD} is the sum of the radiative and non-radiative decay constants k_r and k_{nr} . The PLQE of QD emission (ϕ_{QD}) can then be expressed as the rate of emission, $k_r[QD]$, divided by excitation rate G . Assuming steady-state conditions ($\frac{d[QD]}{dt} = 0$) the expression for ϕ_{QD} can be rearranged to:

$$\phi_{QD} = \frac{k_r[QD]}{k_q[QD] - k_{-q}[Tr] + k_{-TET}[QD] - k_{TET}[L] + k_{QD}[QD]} \quad (S4)$$

With the steady-state approximation and re-arranging the expressions in Equations S1-S3 one can convert Equation S4 to Equation 1 in the main manuscript.

Transient absorption of PM samples

The fluence dependence of the TIPS-Tc triplet lifetime was studied to determine if bimolecular triplet-triplet annihilation (TTA) was an issue. At low fluence ($4 \mu\text{J}/\text{cm}^2$) the bimolecular quenching was deemed negligible as a reasonable fit was obtained using the rate model of Stern *et al.*² where TTA is omitted, Figure S4. Therefore, for the rest of our modelling we neglect any effect of TTA as low fluences were used for all measurements.

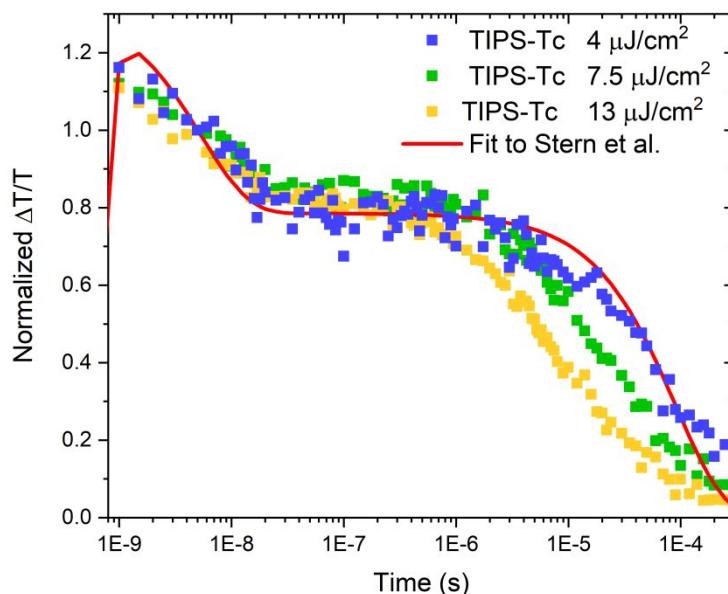


Figure S5. Fluence dependence of TIPS-Tc (200 mg/ml) excited with 515 nm pulses. Fit of low fluence data to rate expressions in Stern *et al* Ref. [7] with the triplet lifetime k_{Tc}^{-1} as free parameter.

Transient absorption maps of all QD/TET-CA's in TIPS-Tc solution are plotted in Figure 3c, d and Figure S6.

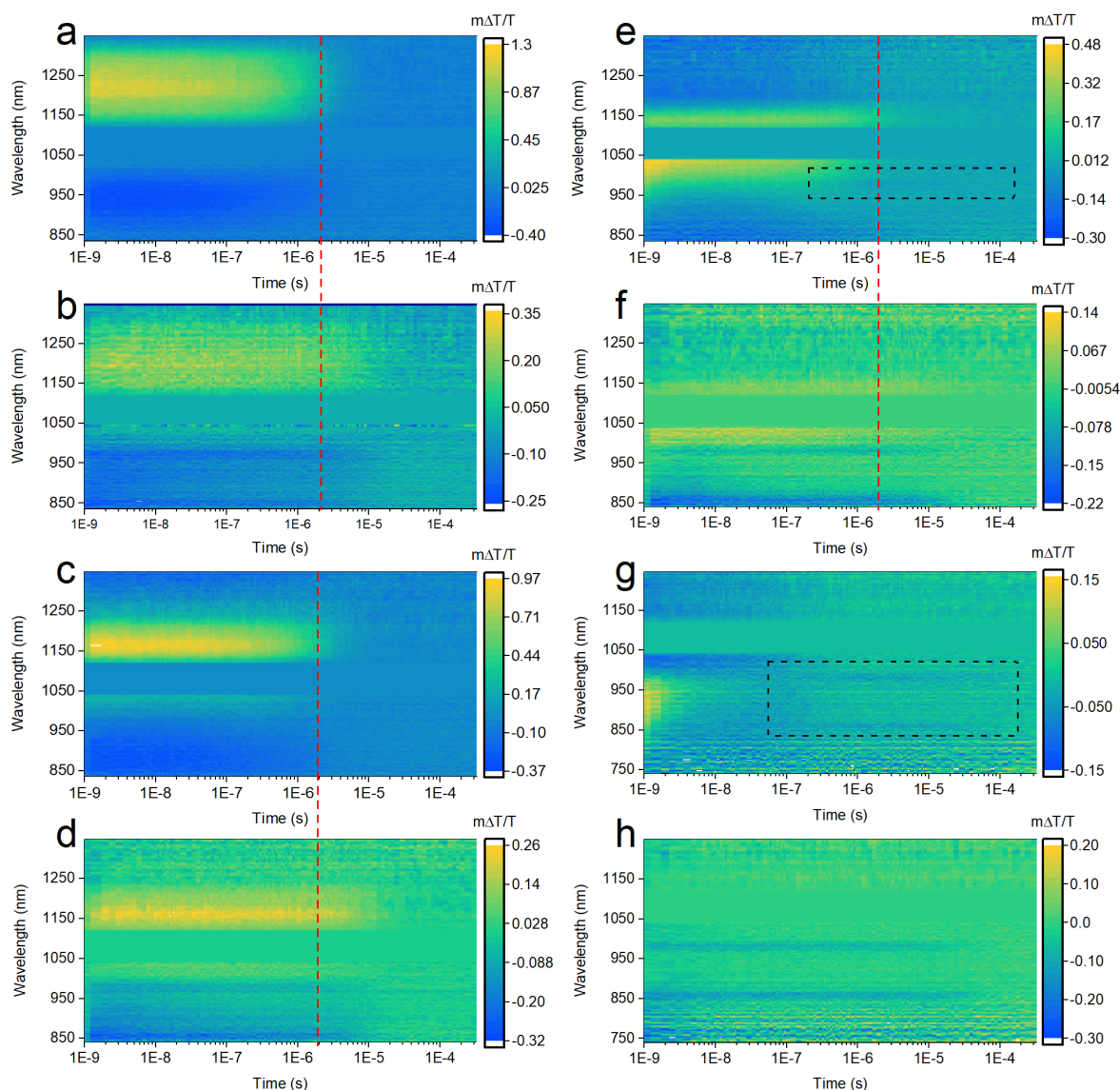


Figure S6. Transient absorption (TA) map of a concentrated TIPS-Tc solution (200 mg/ml) with TET-CA ligated QDs with exciton energies of 1.0 eV (graphs a and b), 1.07 eV (graphs c and d), 1.18 eV (graphs e and f), and 1.30 eV (graphs g and h). Graphs a), c) e) and g) are of samples excited at 650 nm, $3 \mu\text{J}/\text{cm}^2$ whereas graphs b), d), f) and h) from the same samples excited at 515 nm ($4 \mu\text{J}/\text{cm}^2$). Dashed box highlights the TIPS-Tc triplet signal at 860 nm and/or 970 nm. Red dashed lines are a guide for the eye highlighting the extension in QD lifetime in due to triplet transfer from TIPS-Tc.

Decomposition of Triplet and QD features

To decompose the QD/TET-CA and TIPS-Tc features from the TA maps after 515 nm excitation (Figures 3d and S6b, d, f) the spectra of the TIPS-Tc triplets (excitation at 515 nm, Figure 3a) and the corresponding QD/TET-CA spectra (excitation at 650 nm, Figure 3c, and S6a, c, e) were extracted by averaging the spectra over the first 50 ns. Then, the TIPS-Tc and QD/TET-CA spectra were combined in a matrix, **A**, where each row contains the experimentally recorded intensity for TIPS-Tc in the first column and QD/TET-CA in the second column. The kinetic evolution of the spectra were then obtained in a least-square manner by taking the pseudoinverse of matrix **A** times a matrix **D** containing the experimental

TA data. The calculations were carried out in MATLAB® using the `pinv` function. Similar kinetics were obtained for a three spectra deconvolution, also including a **TIPS-Tc** TT spectra, since no significant difference was observed the simpler two spectra decomposition was used. Similarly, the QD/**TET-CA** kinetic after 650 nm excitation (*i.e.* only QD kinetics) were extracted in the same way, but with matrix **A** only containing the QD/**TET-CA** spectra. To obtain the rise in QD/**TET-CA** signal due to triplet transfer from **TIPS-Tc** the QD/**TET-CA** kinetics when excited at 650 nm was subtracted from the QD/**TET-CA** kinetics from the 515 nm excitation. Since there was no triplet transfer in the 1.30 eV QD/**TET-CA** sample (Figure S6g) only the **TIPS-Tc** kinetics were extracted. Figure 4 and S7 shows the extracted kinetics for the various QD energies.

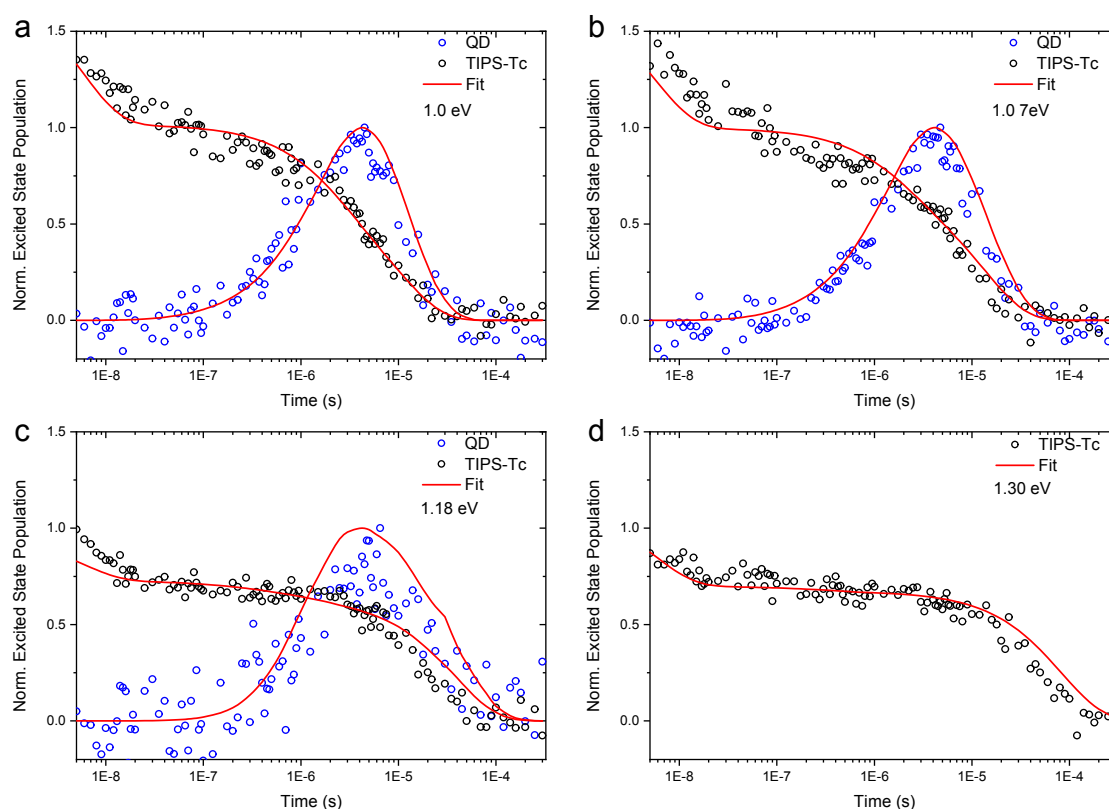


Figure S7. Kinetics of the excited QD and **TIPS-Tc** triplet populations extracted from the TA maps in Figure S6. Solid red lines are fits according to the fitting procedure described below. a) 1.0 eV, b) 1.07 eV, c) 1.18 eV and d) 1.30 eV QDs.

TA of 1.18 eV 1.30 eV QD/**TET-CA** and triplet formation

In Figure S6f and h (black boxes) there is an observable **TIPS-Tc** triplet feature at longer times, even though **TIPS-Tc** has no absorption at the excitation wavelength, 650 nm. The triplet features are an indication that triplet transfer from the QD/**TET-CA** to **TIPS-Tc** does occur. These triplet features are not observed for the lower energy dots, suggesting that 1.18 eV is high enough in energy to, at least partially, populate the ligand triplet, for further triplet transfer to **TIPS-Tc**.

Figure S8 shows the TA map of the 1.30 eV QD/**TET-CA** in toluene excited at 570 nm. After about 500 ns a signal at 540 – 550 nm starts to arise, which we assign to the ligand **TET-CA** triplet state. Considering that the majority of the QD GSB decays in the ps time regime, Figure

S3, and the growth of the **TET-CA** triplet reaches its maximum at 1 μ s there seems to be a delayed transfer from the QD to ligand. Such delayed features have been observed before, and will be reported in detail for the PbS/**TET-CA** in later work. The lifetime of the ligand triplet is obtained by fitting the decay after 1 μ s, Figure S8c, to a monoexponential decay, yielding a 29 μ s time constant.

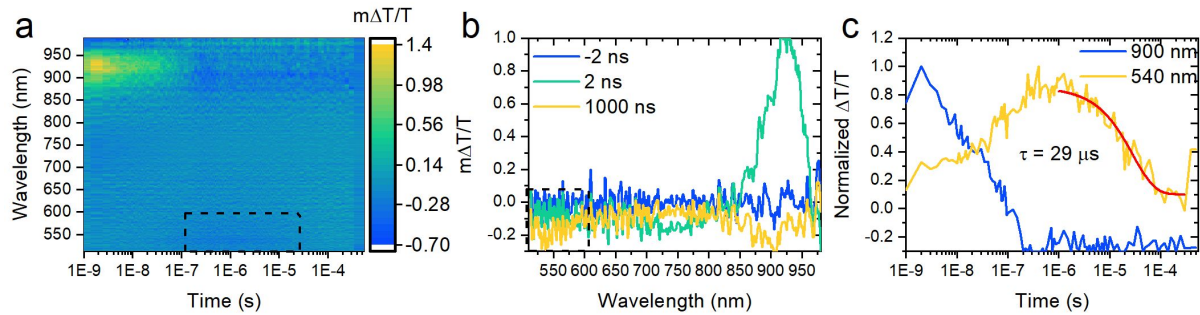


Figure S8. a) TA map of 1.30 eV QD/**TET-CA** in toluene excited at 570 nm (40 nJ/pulse). b) Spectral slices from a) at -2 ns, 2 ns and 1000 ns. Dashed box highlights the ligand **TET-CA** triplet signal. c) Kinetic traces at 900 nm (blue) and 540 nm (yellow). The long time decay at 540 nm is fitted to a monoexponential decay to extract the ligand lifetime of 29 μ s.

Kinetic modelling

Rate equations governing PM

The processes described in Figure 4 can be described by the rate equations in Equations S5-S13. Since the QD has some direct absorption at 515 nm we also add a term for the direct excitation with rate k_{ExQD} .

QD excited state:

$$\frac{d[QD^*]}{dt} = -(k_r + k_{nr})[QD^*] - k_{-TET}[QD^*] - k_q[QD^*] + k_{ExQD}[QD] + k_{TET}[{}^3TET - CA^*] + k_{-q}[Tr] \quad (S5)$$

Ligand triplet:

$$\frac{d[{}^3TET - CA^*]}{dt} = -k_{LD}[{}^3TET - CA^*] - k_{TET}[{}^3TET - CA^*] - k_{-sTET}[{}^3TET - CA^*] + k_{sTET}[{}^1TET - CA] + k_{-TET}[QD^*] \quad (S6)$$

TIPS-Tc singlet:

$$\frac{d[{}^1TIPS - Tc^*]}{dt} = -k_{SD}[{}^1TIPS - Tc^*] - k_{TT}[{}^1TIPS - Tc^*] + k_{Ex}[{}^1TIPS - Tc] \quad (S7)$$

TT state:

$$\frac{d[TT]}{dt} = -k_{SF}[TT] - k_{TTD}[TT] + k_{TT}[{}^1TIPS - Tc^*] \quad (S8)$$

TIPS-Tc triplet state:

$$\frac{d[{}^3TIPS - Tc^*]}{dt} = -k_{TD}[{}^3TIPS - Tc^*] - k_{sTET}[{}^1TET - CA][{}^3TIPS - Tc^*] + k_{-sTET}[{}^3TET - CA^*][{}^1TIPS - Tc] + 2k_{SF}[TT] \quad (S9)$$

QD trap state:

$$\frac{d[\mathbf{Tr}]}{dt} = -k_{-q}[\mathbf{Tr}] - k_{Tr}[\mathbf{Tr}] + k_q[\mathbf{QD}^*] \quad (\text{S10})$$

QD ground state:

$$\frac{d[\mathbf{QD}]}{dt} = -k_{ExQD}[\mathbf{QD}] - k_{TET}[\mathbf{^3TET} - \mathbf{CA}^*] + (k_r + k_{nr})[\mathbf{QD}^*] + k_{-TET}[\mathbf{QD}^*] + k_{Tr}[\mathbf{Tr}] \quad (\text{S11})$$

Ligand Ground state:

$$\frac{d[\mathbf{^1TET} - \mathbf{CA}]}{dt} = k_{LD}[\mathbf{^3TET} - \mathbf{CA}^*] - k_{-TET}[\mathbf{QD}^*] - k_{sTET}[\mathbf{^1TET} - \mathbf{CA}][\mathbf{^3TIPS} - \mathbf{Tc}^*] + k_{TET}[\mathbf{^3TET} - \mathbf{CA}^*] + k_{-sTET}[\mathbf{^3TET} - \mathbf{CA}^*][\mathbf{^1TIPS} - \mathbf{Tc}] \quad (\text{S12})$$

TIPS-Tc ground state:

$$\frac{d[\mathbf{^1TIPS} - \mathbf{Tc}]}{dt} = -k_{TT}[\mathbf{^1TIPS} - \mathbf{Tc}^*] - k_{Ex}[\mathbf{^1TIPS} - \mathbf{Tc}] - k_{-sTET}[\mathbf{^3TET} - \mathbf{CA}^*][\mathbf{^1TIPS} - \mathbf{Tc}] + 2k_{TTD}[\mathbf{TT}] + k_{SD}[\mathbf{^1TIPS} - \mathbf{Tc}^*] + k_{sTET}[\mathbf{^1TET} - \mathbf{CA}][\mathbf{^3TIPS} - \mathbf{Tc}^*] + k_{TD}[\mathbf{^3TIPS} - \mathbf{Tc}^*] \quad (\text{S13})$$

Fitting procedure

Rates describing the SF process were taken from Stert *et al.*,² although a slightly larger SF rate k_{SF} was used. The rates for QD decay (k_r+k_{nr}), **TIPS-Tc** triplet decay (k_{TD}), ligand decay (k_{LD}), were taken from the experimental fitting discussed above and in the main manuscript. An average trapping rate of 1/100 ps⁻¹ was used as it was within the range estimated from the ps-TA quenching, Figure S3. The Rates for repopulation of the QD from the trap (k_q) and the trap decay (k_{Tr}) were obtained by calculating the steady-state PLQE of the ligand exchanged dots according to Equation 1, and finding the best agreement to the 3 low energy dots (negligible QD-to-ligand triplet transfer k_{-TET}).

After assuming a diffusion limited k_{sTET} and the corresponding reverse rate k_{-sTET} ($k_{-sTET} = k_{TET} \exp(-\frac{\Delta E}{k_b T})$; $\Delta E = 0.1$ eV) there remains 2 unknowns, k_{TET} and k_{-TET} . These rate constants were used as free variables in the fitting to the deconvoluted kinetics. The differential equations S5-S13 were solved numerically over the experimental time range using MATLAB® built-in function `ode23s`. The extracted population dynamics for the **TIPS-Tc** triplet and TT state as well as the QD excited state were normalized and compared to the experimental deconvoluted kinetic traces for 515 nm excitation. The sum of residuals was used as the minimization value to obtain the best fit with the rate constants k_{TET} and k_{-TET} as the fitting parameters.

In the same minimization function the rate equations were also solved for steady-state with the same k_{TET} and k_{-TET} to calculate the PLQE for 515 nm and 658 nm excitation, if the estimated PLQE values differed by 20% or more from the experimental values the sum of residuals was multiplied by 1×10^6 to force the minimization to find k_{TET} and k_{-TET} values that gave the best fit to the kinetics while also reproducing reasonable PLQE values.

The PLQEs for 515 nm and 658 nm excitation, φ_{515nm} and φ_{658nm} , respectively, were calculated according to Equations S14 and S15.

$$\varphi_{515nm} = \frac{\varphi_{QD} k_{QD}[\mathbf{QD}^*]}{k_{Ex-ss}[\mathbf{TIPS} - \mathbf{Tc}] + k_{ExQD-515nm}[\mathbf{QD}]} \quad (\text{S14})$$

$$\varphi_{658nm} = \frac{\varphi_{QD}k_{QD}[QD^*]}{k_{ExQD-658nm}[QD]} \quad (S15)$$

Here k_{Ex-ss} , $k_{ExQD-515nm}$ and $k_{ExQD-658nm}$ are the excitation rates (s^{-1}) under the experimental conditions for the steady-state PLQE measurements (Table S1) for direct absorption of **TIPS-Tc** at 515 nm, the QD at 515 nm and the QD at 658 nm excitation, respectively. In the case for 515 nm excitation the rates are corrected for the competitive absorption of both components based on the absorption of the actual samples.

The SF yield, η_{SF} , is defined as the number of free triplets generated per absorbed photon, and can be calculated according to Equation S16.

$$\eta_{SF} = \frac{2k_{SF}[TT]}{k_{Ex-ss}[TIPS-Tc]} \quad (S16)$$

Fitting results and error estimate

Table 1 in the main text lists all the rate constants used in the fitting, free variables estimated from the fitting are in bold font, and the rest were fixed to the values in the table. Fits to the deconvoluted data are shown in Figure S7. The obtained rate constants are also plotted as a function of energetic driving force in Figure 5 and S9.

The error of the fit was estimated by varying k_{TET} and k_{-TET} by 2 orders of magnitude and monitoring the interval where the sum of residuals stayed within 5% of the minimized value. Similar to the fitting procedure, the steady-state PLQE values were estimated and compared to the experimental PLQE values, if the PLQE's differed by more than 20% the error was considered to be outside the 5% criteria.

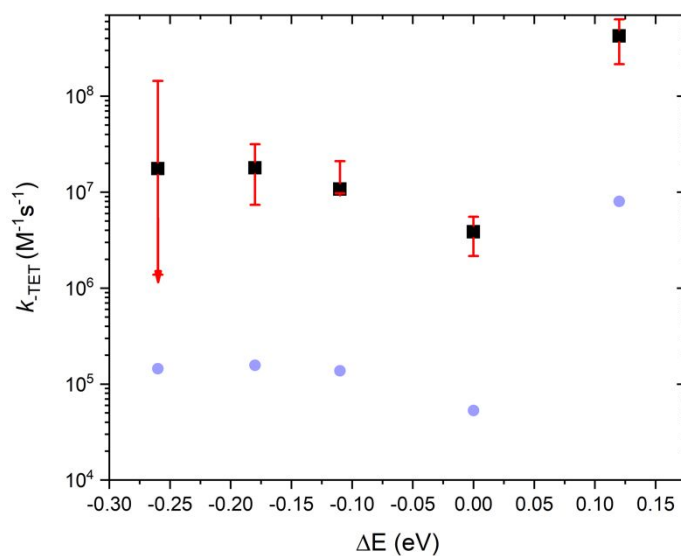


Figure S9. Obtained k_{TET} rate constants for the triplet transfer from QD to ligand (black squares), with error estimates. As the triplet transfer process for the lowest energy dot is not rate limiting the estimated error is large, as illustrated by the arrow on the error bar an even lower value would still result in an acceptable fitting. Blue circles are the k_{TET} rate constants normalized by number of ligands/QD.

References

- (1) Moreels, I.; Lambert, K.; Muynck, D. De; Vanhaecke, F.; Poelman, D.; Martins, J. C.; Allan, G.; Hens, Z. Size-Dependent Optical Properties of Colloidal PbS Quantum Dots. *ACS Nano* **2009**, *3*, 3023–3030.

- (2) Stern, H. L.; Musser, A. J.; Gelinas, S.; Parkinson, P.; Herz, L. M.; Bruzek, M. J.; Anthony, J.; Friend, R. H.; Walker, B. J. Identification of a Triplet Pair Intermediate in Singlet Exciton Fission in Solution. *Proc. Natl. Acad. Sci.* **2015**, *112*, 7656–7661.